CHEMISTRY
A EUROPEAN JOURNAL

DOI: 10.1002/chem.200903078

Energetics, Conformation, and Recognition of DNA Duplexes Modified by Monodentate Ru^{II} Complexes Containing Terphenyl Arenes

Olga Novakova,[a] Jaroslav Malina,[a] Tereza Suchankova,[b] Jana Kasparkova,[a] Tijana Bugarcic,[c] Peter J. Sadler,[c] and Viktor Brabec*[a]

Abstract: We studied the thermodynamic properties, conformation, and recognition of DNA duplexes site-specifically modified by monofunctional adducts of Ru^{II} complexes of the type $[Ru^{II}(\eta^6\text{-arene})(Cl)(en)]^+$, in which arene = *para*-, *meta*-, or *ortho*-terphenyl (complexes **1**, **2**, and **3**, respectively) and en = 1,2-diaminoethane. It has been shown (*J. Med. Chem.* **2008**, *51*, 5310) that **1** exhibits promising cytotoxic effects in human tumor cells, whereas **2** and **3** are much less cytotoxic; concomitantly with the high cytotoxicity of **1**, its DNA binding mode involves combined intercalative and monofunctional (coordination) binding modes, whereas less cytotoxic compounds **2** and **3** bind to DNA only through a monofunctional coordination to DNA bases. An analysis of conformational distortions induced in DNA by adducts of **1** and **2** revealed more extensive and stronger distortion and concomitantly greater thermodynamic destabilization of DNA by the adducts of nonintercalating **2**. Moreover, affinity of replication protein A to the DNA duplex containing adduct of **1** was pronouncedly lower than to the adduct of **2**. On the other hand, another damaged-DNA-binding protein, xeroderma pigmentosum protein A, did not recognize the DNA adduct of **1** or **2**. Importantly, the adducts of **1** induced a considerably lower level of repair synthesis than the adducts of **2**, which suggests enhanced persistence of the adducts of the more potent and intercalating **1** in comparison with the adducts of the less potent and nonintercalating **2**. Also interestingly, the adducts of **1** inhibited DNA polymerization more efficiently than the adducts of **2**, and they could also be bypassed by DNA polymerases with greater difficulty. Results of the present work along with those previously published support the view that monodentate Ru^{II} arene complexes belong to a class of anticancer agents for which structure–pharmacological relationships might be correlated with their DNA-binding modes.

Keywords: arenes · calorimetry · DNA · DNA recognition · ruthenium

Introduction

Ruthenium complexes have attracted much interest as alternative drugs to cisplatin (*cis*-diamminedichloridoplatinum(II)) and its analogues in cancer chemotherapy. Organometallic Ru^{II}–arene complexes of the type $[Ru^{II}(\eta^6\text{-arene})(Cl)(en)][PF_6]$ (en = 1,2-diaminoethane) constitute a relatively new group of anticancer compounds.[1–4] These monodentate complexes appear to be novel anticancer agents with a mechanism of action different from those of platinum and other ruthenium complexes that have been tested for antitumor activity. Although the pharmacological target for antitumor ruthenium compounds has not been unequivocally identified, there is a large body of evidence indicating that the cytotoxicity of several ruthenium complexes correlates with their ability to bind DNA,[5] although several exceptions have been reported.[6,7] Because the Ru^{II}–arene complexes bind strongly to DNA,[8–15] DNA modifications

[a] Dr. O. Novakova, Dr. J. Malina, Dr. J. Kasparkova, Prof. Dr. V. Brabec
Institute of Biophysics
Academy of Sciences of the Czech Republic, v.v.i., Kralovopolska 135
61265 Brno (Czech Republic)
Fax: (+420) 541240499
E-mail: brabec@ibp.cz

[b] T. Suchankova
Laboratory of Biophysics
Department of Experimental Physics, Faculty of Sciences
Palacky University
771 46 Olomouc (Czech Republic)

[c] Dr. T. Bugarcic, Prof. Dr. P. J. Sadler
Department of Chemistry
University of Warwick
Coventry C4V 7AL (UK)

Supporting information for this article is available on the WWW under http://dx.doi.org/10.1002/chem.200903078.

and the downstream effects of these modifications are of great interest. It has been shown that Ru^{II}–arene complexes of the type $[Ru^{II}(\eta^6\text{-arene})(Cl)(en)][PF_6]$ can form monofunctional adducts with DNA at guanine residues. Some of these Ru^{II} complexes, in particular those containing multiring arenes, bind to DNA not only through coordination to the N7 atoms of guanine (G), but also noncovalently through hydrophobic interactions between the arene and DNA.[9,10,13] These hydrophobic interactions might include intercalation of the noncoordinated arenes between DNA bases and minor-groove binding.

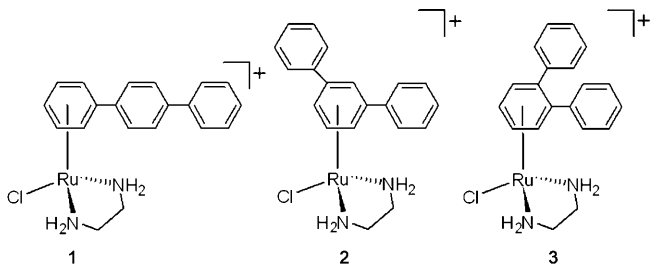

Recently, new complexes of the type $[Ru^{II}(\eta^6\text{-arene})(Cl)(en)]^+$ (arene = *ortho*-, *meta*-, or *para*-terphenyl) have been synthesized to investigate the effect on cytotoxicity and DNA binding of structural isomerization of the multiring terphenyl arene ligand.[13] Importantly, the complex containing *para*-terphenyl as the arene ligand (complex **1**) exhibits promising cytotoxic effects in several human tumor cell lines, including those resistant to conventional cisplatin. In contrast, complexes containing *meta*- or *ortho*-terphenyl arene ligands (complexes **2** and **3**, respectively) are much less cytotoxic. Complexes **1** and **2** were selected for an initial study focused on global modification of natural, high-molecular-mass DNA.[13] The results of this study have revealed that, concomitant with the relatively high cytotoxicity of **1** in tumor cells, its DNA-binding mode involves combined intercalative and monofunctional (coordination) binding modes. In contrast, complex **2**, which is much less cytotoxic, binds to DNA through only a monofunctional coordination to DNA bases. Therefore, the results of our initial work[13] have further supported the view that the presence of the arene ligand in $[Ru(\eta^6\text{-arene})(Cl)(en)]^+$ complexes capable of noncovalent, hydrophobic interaction with DNA considerably enhances cytotoxicity in tumor cell lines.

Herein, we have studied the thermodynamic properties, conformation, and recognition of DNA duplexes uniquely and site-specifically modified by the two monodentate Ru^{II}–arene complexes $[Ru^{II}(Cl)(en)(\eta^6\text{-}p\text{-terphenyl})]^+$ (**1**) and $[Ru^{II}(Cl)(en)(\eta^6\text{-}m\text{-terphenyl})]^+$ (**2**) to elucidate in detail the DNA-binding mode of these Ru^{II} arene complexes. We compare previously obtained cytotoxicity data[13] with new data obtained in the present work on conformational distortions induced by single, site-specific monofunctional adducts of the Ru^{II} in short oligodeoxyribonucleotide duplexes, associated alterations in the thermodynamic stability of these duplexes, recognition and repair of these adducts by two specific proteins, that is, the important factors that modulate the antitumor effects of antitumor metallodrugs already used in clinic.

Results

Differential scanning calorimetry (DSC) and thermal stability of ruthenated DNA duplexes: Previous studies have demonstrated that DSC is a very useful tool to characterize the thermodynamic stability of DNA duplexes containing adducts of various antitumor metallodrugs.[10,16–25] Therefore, our initial studies characterizing the effect of the monofunctional adducts of complexes **1** and **2** on the thermal stability and energetics of DNA duplexes were performed by using DSC. As in our previous studies, we analyzed the 15 bp DNA duplexCAL (its nucleotide sequence is shown in Figure 1D) site-specifically modified by complexes **1** or **2**. DSC makes it possible to measure excess heat capacity versus temperature profiles for the thermally induced transitions of nonmodified DNA duplexes and those containing a unique adduct of the metal-based drug. Thermograms were recorded with the heating rate of $60\,K\,h^{-1}$, and after reaching the maximum temperature of 368 K, the samples were cooled at the same rate to the starting temperature of 288 K. Inspection of the thermograms of the ruthenated duplexes revealed that the first scans differed markedly from the following scans, which were superimposable with the melting profile of the nonmodified duplex. The duplexes containing unique Ru^{II} adducts were exposed to higher temperatures during the first scan for a relatively long period of time (for instance, for 90 min to temperatures $\geq$323 K). A plausible explanation of the DSC results might be that the adducts of complexes **1** and **2** were unstable at higher temperatures (Ru^{II} complexes dissociated from their DNA-binding sites during the first scan so that the following melting profiles coincided with that of the nonmodified duplex). Therefore, we first verified the stability of the adducts of complexes **1** and **2** at various temperatures. Consistent with previous findings,[26] we found that these adducts formed in the duplexCAL were stable for more than 12 h only at temperatures lower than 333 K. Therefore, it is apparent that DSC cannot be used to analyze duplexes containing the adducts of these two Ru^{II} arene complexes.

Isothermal titration calorimetry (ITC): ITC represents a suitable alternative that makes it possible to study the thermodynamic parameters of the duplex formation from its two complementary single strands over a range of temperatures, including relatively low temperatures at which the DNA adducts of Ru^{II} arene compounds are stable for long enough to complete the ITC experiment. Representative examples of ITC profiles of duplexCAL formation from its nonmodified bottom strand titrated into the complementary nonmodified top strand or into the same strand containing a single monofunctional adduct of **1** or **2** at 293 K are depicted

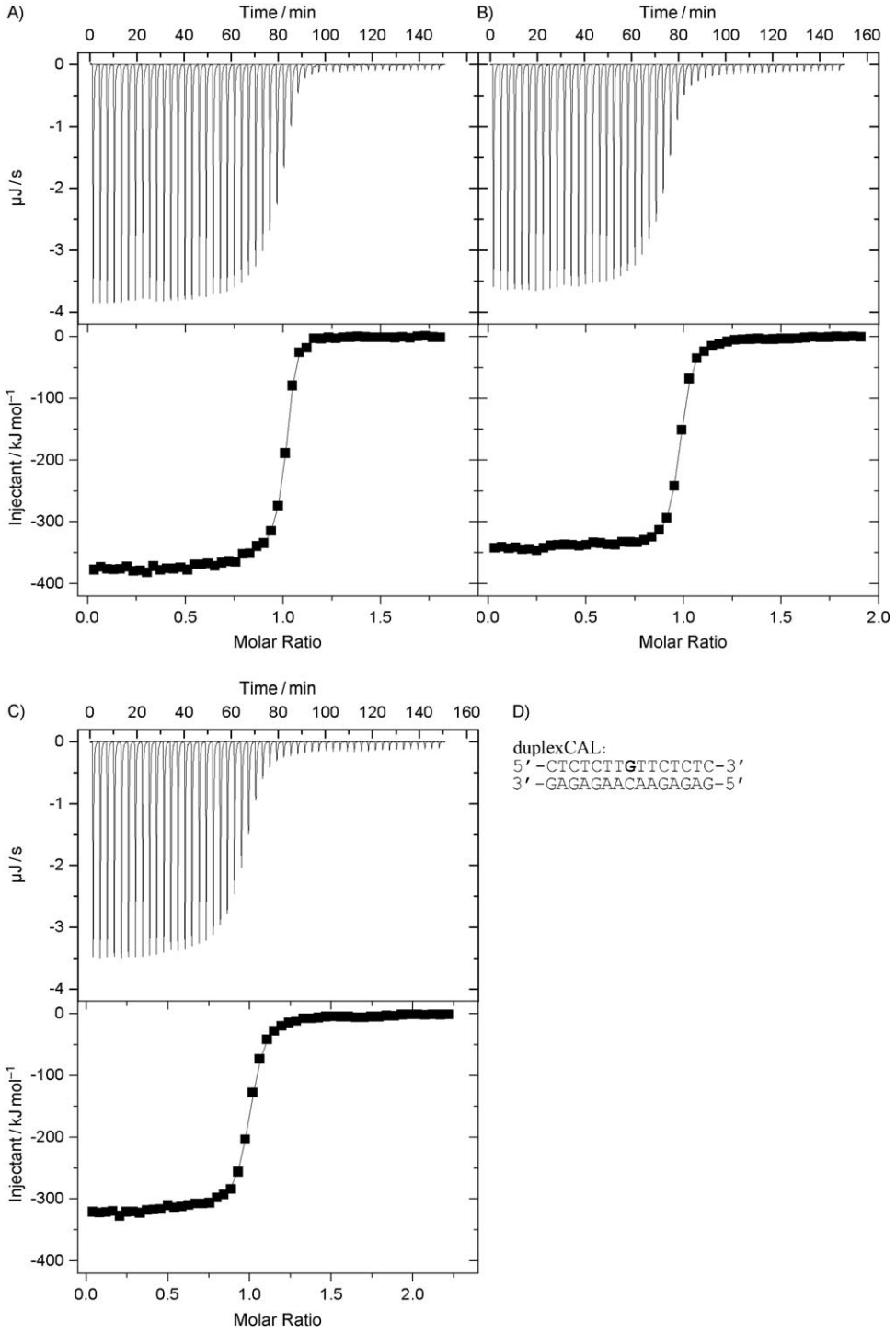

Figure 1. ITC binding isotherms for the association of the top strand of the 15 bp duplexCAL (nucleotide sequence shown in D) for A) nonmodified duplex and B,C) a duplex containing a single, monofunctional adduct of **1** or **2**, respectively, with the complementary (nonmodified) strand (bottom strand at 293 K) in phosphate buffer (10 mM, pH 7.0) containing NaCl (50 mM). The upper panels in A)–C) show the total heat released upon injecting 5 µL aliquots of the bottom strand (50 µM) into a 1.4 mL reaction cell containing the top strand (5 µM). The lower panels show the resultant binding isotherms (■) obtained by integrating the peak areas of each injection; —— represents the nonlinear least squares fit of the enthalpy change (ΔH), entropy change (ΔS), stoichiometry (n), and equilibrium constant (K) for strand association to a single-site binding model. For other details, see the text. D) Sequence of the 15 bp duplexCAL used in the calorimetric experiments; the central **G** residue in the top strand indicates the location of the monofunctional adduct of the Ru^{II} arene complex.

in Figure 1A, B, and C, respectively. The same measurements were performed also at 298, 303, and 310 K. The ITC profiles were analyzed to obtain the thermodynamic parameters listed in Table 1. Thermodynamic data for the association of strands modified by **2** at 310 K could not be obtained because the presence of the monofunctional adduct of this Ru^{II}–arene complex lowered the melting temperature of the duplexCAL so that the duplex partially melted at 310 K. Figure 2 shows the dependence of the thermodynamic parameters K, ΔH, $T\Delta S$, and ΔG on the temperature.

The values of ΔH (Figure 2B) and $T\Delta S$ (Figure 2C) obtained for association of complementary non-modified strands of duplexCAL were almost independent of the temperature. Consequently ΔG (Figure 2D), calculated by using the standard thermodynamic relationship $\Delta G = \Delta H - T\Delta S$, increased only slightly with increasing temperature from $-46.9\ kJ\,mol^{-1}$ at 293 K to $-43.1\ kJ\,mol^{-1}$ at 310 K. The equilibrium constant for the strand association (K) depended strongly on the temperature and decreased steeply with increasing temperature from $2.26\times10^{8}\ M^{-1}$ at 293 K to $1.74\times10^{7}\ M^{-1}$ at 310 K, which is more than an order of magnitude over a 17 K temperature range.

Inspection of the thermodynamic parameters revealed that the exothermic formation of the single monofunctional adduct in the duplexCAL by complexes **1** and **2** enthalpically destabilized the duplexCAL relative to its nonmodified counterpart at 293 K ($\Delta\Delta H =$ 38.0 and 58.2 $kJ\,mol^{-1}$, respectively). In addition, the formation of monofunctional adducts by **1** and **2** resulted in a substantial increase in the entropy

Table 1. Calorimetrically derived thermodynamic parameters for the formation of the 15 bp duplexCAL unmodified or containing a single site-specific monofunctional adduct of **1** or **2** at 293, 298, 303, and 310 K.[a]

	ΔH [kJ mol^{-1}]	$T\Delta S$ [kJ mol^{-1}]	ΔG [kJ mol^{-1}]	K [M^{-}]	n	$\Delta\Delta H$ [kJ mol^{-1}]	$T\Delta\Delta S$ [kJ mol^{-1}]	$\Delta\Delta G$ [kJ mol^{-1}]
293 K								
control	−379.2	−332.3	−46.9	2.26×10^{8}	0.98			
1	−341.2	−294.6	−46.6	1.96×10^{8}	0.98	38.0	37.7	0.3
2	−321.0	−276.0	−45.0	9.77×10^{7}	0.99	58.2	56.3	1.9
298 K								
control	−378.0	−331.6	−46.5	1.36×10^{8}	1.00			
1	−343.9	−298.0	−46.0	1.11×10^{8}	0.99	34.1	33.6	0.5
2	−322.9	−279.6	−43.3	3.70×10^{7}	1.00	55.1	52.0	3.2
303 K								
control	−376.9	−331.8	−45.2	5.76×10^{7}	1.00			
1	−346.9	−302.4	−44.5	4.45×10^{7}	1.00	30.0	29.4	0.7
2	−324.9	−283.7	−41.2	1.24×10^{7}	0.98	52.0	48.1	4.0
310 K								
control	−379.1	−336.0	−43.1	1.74×10^{7}	0.99			
1	−351.9	−308.0	−43.9	2.42×10^{7}	0.98	27.2	28.0	−0.8

[a] ΔH, ΔS, and ΔG denote the enthalpy, entropy, and free energy (at corresponding temperature), respectively, of duplex formation. K and n denote the association constant and binding stoichiometry, respectively, for strand association. $\Delta\Delta$ parameters are computed by subtracting the appropriate value measured for the control, unmodified duplex from the value measured for the duplex containing the single, site-specific ruthenium adduct.

of the duplexCAL ($T\Delta\Delta S = 37.7$ and 56.3 kJ mol^{-1}, respectively). In other words, the monofunctional adducts of **1** and **2** increased the entropy of the ruthenated duplexes and, in this way, entropically stabilized the duplex. Thus, the enthalpic destabilization of the duplexCAL due to the monofunctional adduct of **1** and **2** is partially, but not completely, compensated by the entropic stabilization of the duplex induced by these adducts. The net result of these enthalpic and entropic effects is that the formation of the monofunctional adducts of **1** and **2** with the duplexCAL induced a decrease of duplex thermodynamic stability at 293 K ($\Delta\Delta G$) of 0.3 and 1.9 kJ mol^{-1}, respectively, with this destabilization being enthalpic in origin. However, the effect of monofunctional adducts of **1** and **2** on the thermodynamic stability of the duplex changed with increasing temperature.

The enthalpic destabilization ($\Delta\Delta H$) of duplexCAL induced by adduct formation with **1** decreased with increasing temperature from 38.0 kJ mol^{-1} at 293 K to 27.2 kJ mol^{-1} at 310 K. The entropic stabilization ($T\Delta\Delta S$) compensating the enthalpic destabilization also decreased from 37.7 to 28.0 kJ mol^{-1} over this temperature range. The net result of these enthalpic and entropic effects was that the presence of the monofunctional adduct of **1** had little effect on the thermodynamic stability (ΔG) of duplexCAL. The values of $\Delta\Delta G$ were 0.3, 0.5, 0.7, and −0.8 kJ mol^{-1} at 293, 298, 303, and 310 K, respectively. The slope of the linear least-squares fit to the dependence of the binding enthalpy (ΔH) on the temperature in Figure 2B gave a negative heat capacity change for duplexCAL formation, ΔC_p, of (-632 ± 29) J K^{-1} mol^{-1}. The values of the association constant (K) were very close to the association constants of the nonmodified strands at all temperatures. Interestingly, at 310 K the association constant K reached a value of 2.42×10^{7} M^{-1}, which was only slightly higher than that of nonmodified strands (1.74×10^{7} M^{-1}). The entropic stabilization at 310 K ($T\Delta\Delta S = 28.0$ kJ mol^{-1}) was higher than the enthalpic destabilization ($\Delta\Delta H = 27.2$ kJ mol^{-1}), which implies that the adduct of **1** induced a slight increase in the thermodynamic stability of duplexCAL ($\Delta\Delta G = -0.8$ kJ mol^{-1}), with this stabilization being entropic in origin.

The adduct of duplexCAL with **2** behaved similarly to the duplex modified by **1**. The enthalpic destabilization ($\Delta\Delta H$) of duplexCAL induced by for-

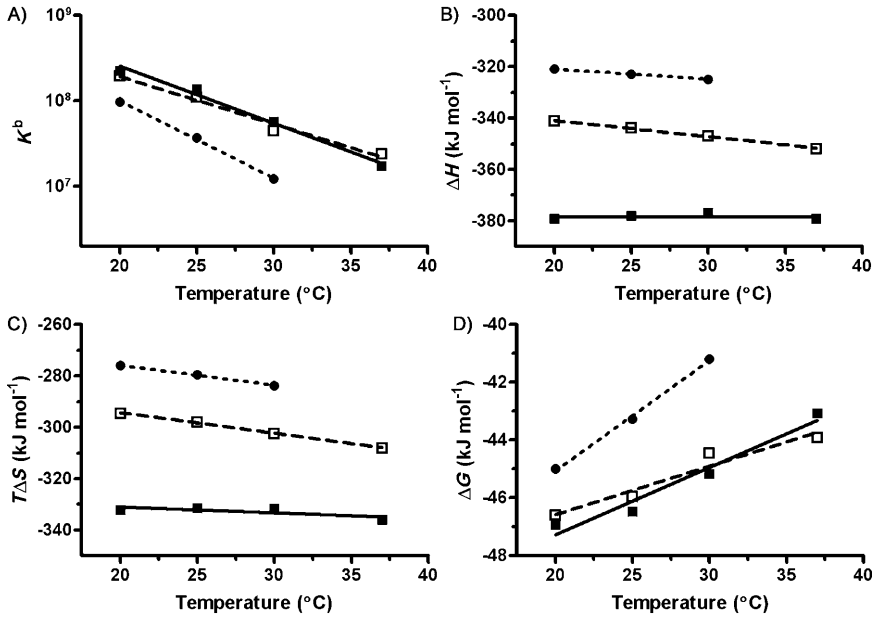

Figure 2. The variations in A) K, B) ΔH, C) $T\Delta S$, and D) ΔG with temperature. ■: control, nonmodified duplexCAL; □: duplexCAL containing monofunctional adduct of **1**; ●: duplexCAL containing monofunctional adduct of **2**. For other details, see Figure 1 and the text.

mation of an adduct with **2** decreased with increasing temperature. The entropic stabilization ($T\Delta\Delta S$) also decreased with temperature, but the reduction was more pronounced and resulted in a decrease in the thermodynamic stability ($\Delta\Delta G$) of the duplex with increasing temperature from 1.9 kJ mol^{-1} at 293 K to 4.0 kJ mol^{-1} at 303 K. The binding enthalpy (Figure 2B) exhibited a decrease with increase in temperature, giving a negative heat capacity change (ΔC_p) of (-394 ± 8) kJ K^{-1} mol^{-1}. The association constants (K) range from 9.77×10^7 M^{-1} at 293 K to 1.24×10^7 M^{-1} at 303 K, which is approximately 2–4 times lower than the association constants of the non-modified strands.

Chemical probes for DNA conformation: We previously demonstrated that complexes **1** and **2** bind preferentially to G residues in natural double-helical DNA to form monofunctional adducts.[13] To obtain information on how these adducts affect DNA conformation, oligonucleotide duplexes containing a site-specific monofunctional adduct of **1** or **2** at the G residue were further analyzed by chemical probes of DNA conformation. The ruthenated 15 bp duplex (duplexCAL) was treated with two chemical agents, $KMnO_4$ and diethylpyrocarbonate (DEPC), which are used as tools for monitoring the existence of conformations other than canonical B DNA. They react preferentially with single-stranded DNA and distorted double-stranded DNA.[27,28] For this analysis, we used exactly the same methodology as in our recent studies dealing with DNA adducts of various antitumor platinum drugs (for example, see refs. [28,29] for the details of this experiment), and representative gels showing piperidine-induced specific strand cleavage at $KMnO_4$-modified and DEPC-modified bases in the unruthenated 15 bp duplex or the duplex-containing the single monofunctional adduct of **1** or **2** are illustrated in Figure S1 in the Supporting Information. The results are schematically summarized in Figure 3. The pattern and degree of reactivity toward the chemical probes found for the adducts of **1** and **2** indicate that the distortion induced by the adduct of complex **1** was markedly less extensive than that induced by the adduct of **2**.

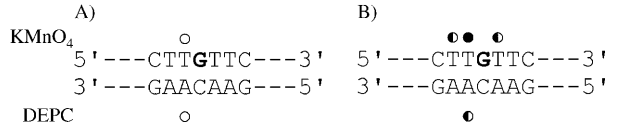

Figure 3. Summary of the reactivity of chemical probes with 15 bp duplexCAL containing a monofunctional adduct of **1** (A) or **2** (B). Filled, half-filled, and empty circles designate strong, medium, and weak reactivity, respectively.

Recognition of the duplexes containing adducts of Ru^{II}–arene complexes by RPA and XPA proteins: Having characterized the effects of the monofunctional adducts of complexes **1** and **2** on thermodynamics of the DNA duplexCAL, we have employed an electrophoretic mobility shift assay (EMSA) to determine how replication protein A (RPA) and xeroderma pigmentosum group A protein (XPA) interact with DNA that has been damaged by these monofunctional adducts. Substrates (30 bp) were designed to contain a single, site-specific monofunctional adduct of **1** or **2** in the 15 bp central sequence, identical to that of the 15 bp duplexCAL used for calorimetric measurements. The sequences in these longer 30 bp duplexes (duplexesEMSA) on both sides of the central TGT sequences were chosen to contain only thymines and cytosines in the top strands and adenines and guanines in the bottom strands.

Under the conditions determined to minimize RPA binding to undamaged DNA,[30] increasing concentrations of RPA were employed in an EMSA to examine duplexesEMSA in the presence or absence of single, site-specific monofunctional adduct of **1** or **2** (Figure 4). Quantification

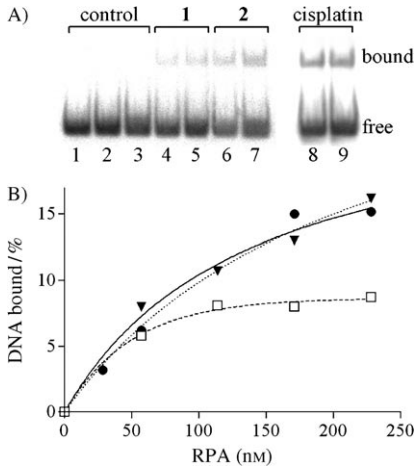

Figure 4. A) RPA binding of undamaged 30 bp duplexesEMSA (lanes 1–3) or the duplexesEMSA containing a monofunctional adduct of **1** (lanes 4, 5), **2** (lanes 6, 7), or 1,2-GG intrastrand crosslink of cisplatin (lanes 8, 9). EMSAs were performed by using no added RPA (lane 1), 171 nM RPA (lanes 2, 4, 6, and 8), or 228 nM RPA (lanes 3, 5, 7, and 9). The products were separated on 6% native polyacrylamide (PAA) and visualized by using autoradiography. B) Quantification of increasing concentrations of RPA binding to a duplex containing a 1,2-GG intrastrand crosslink of cisplatin (○) or a monofunctional adduct of **1** (□) or **2** (▼). The results are the average of two individual experiments.

of the gels (some representative reactions are shown Figure 4A) shows that RPA bound to the duplexEMSA that contained the adduct of **1** with approximately half the affinity of that containing the adduct of **2** (Figure 4B). It was also verified (not shown) that RPA did not bind to the unmodified duplexEMSA even at the highest concentration of the protein (228 nM) used in these experiments.

Results showing XPA protein binding to a duplexEMSA identical to those used in the experiments demonstrating RPA binding are presented in Figure 5. Lanes 1–3 in Figure 5A represent the control undamaged duplexEMSA and revealed only a very low level of XPA protein binding compared with the duplex containing a 1,2-GG intrastrand adduct of cisplatin in lanes 4–6. Quantification of the gels shows a 4.2-fold increase in XPA protein binding to the

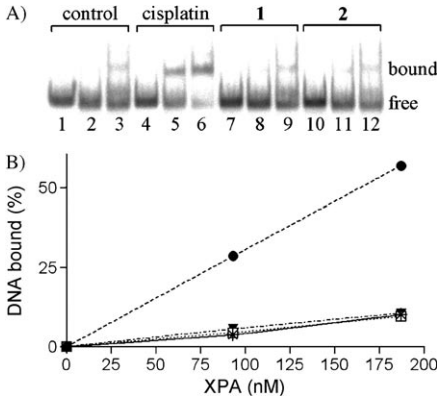

Figure 5. A) XPA binding of undamaged 30 bp duplexesEMSA (lanes 1–3), or the duplexesEMSA containing a 1,2-GG intrastrand crosslink of cisplatin (lanes 4–6) or a monofunctional adduct of **1** (lanes 7–9) or **2** (lanes 10–12). EMSAs were performed by using no added XPA (lanes 1, 4, 7, and 10), 93 nM XPA (lanes 2, 5, 8, and 11), or 187 nM XPA (lanes 3, 6, 9, and 12). The products were separated on 6% native PAA and visualized by autoradiography. B) Quantification of increasing concentrations of XPA binding to the undamaged duplex (∗), the duplex containing a 1,2-GG intrastrand crosslink of cisplatin (●), a monofunctional adduct of **1** (□) or **2** (▼). The results are the average of two individual experiments.

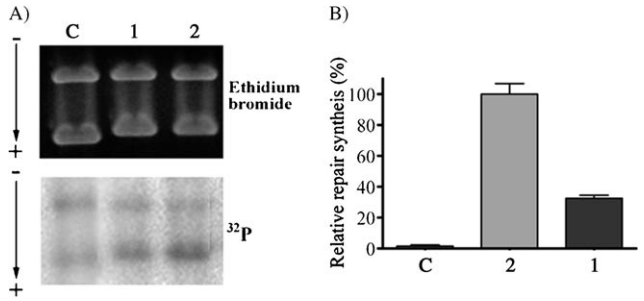

Figure 6. In vitro DNA repair synthesis assay of an extract prepared from the repair-proficient HeLa cell line. Repair synthesis used pBR322 plasmids (nonmodified) plus pUC19 plasmids (nonmodified (lane C) or modified at $r_b = 0.03$ by **1** (lane 1) or **2** (lane 2)) as substrates. A) Results of a typical experiment. Top: a photograph of the EtBr-stained gel; bottom: an autoradiogram of the gel showing incorporation of [α-^{32}P]dCMP. B) Incorporation of dCMP into a nonmodified or ruthenated pUC19 plasmid. For all quantifications representing mean values of three separate experiments, incorporation of radioactive material is corrected for the relative DNA content in each band. The radioactivity associated with the incorporation of [α-^{32}P]dCMP into DNA modified by **1** was taken as 100%. Bars indicate the standard error of the mean (SEM).

duplex containing 1,2-intrastrand adduct of cisplatin compared with the undamaged control (Figure 5B). Interestingly, a very low binding of XPA protein was evident for the duplexEMSA containing a monofunctional adduct of **1** or **2** comparable to the unmodified duplex.

DNA repair synthesis by human cell extract: DNA repair efficiency in a pUC19 plasmid (2686 bp) globally modified by **1** or **2** at $r_b = 0.03$ was tested by using cell-free extract (CFE) of repair-proficient HeLa cells (r_b is defined as the number of molecules of the Ru^{II}–arene complex bound per nucleotide residue). Repair activity was monitored by measuring the amount of incorporated radiolabeled nucleotide. The incorporation of radioactive material was corrected for the relative DNA content in each band. As illustrated in Figure 6, damage-induced DNA repair synthesis detected in the plasmid modified by **1** was only approximately 30% of that found for the plasmid modified by **2** at the same level of modification.

Inhibition of DNA polymerization: It has been demonstrated that DNA modifications by various transition-metal-based complexes have significant effects on the activity of a number of prokaryotic, eukaryotic, and viral DNA polymerases.[31–37] Interestingly, for DNA templates containing site-specifically placed adducts of various platinum compounds, a number of prokaryotic and eukaryotic DNA polymerases are blocked, but others can traverse through platinum adducts depending on their character and conformational alterations induced in the DNA. It is, therefore, of great interest to examine whether DNA polymerases that process DNA substrates containing monofunctional adducts of **1** or **2** can reveal potential differences in alterations imposed on DNA by adducts of these two Ru^{II} arene complexes with different nonleaving arene ligands.

Herein, we investigate DNA polymerization by using templates site-specifically modified by the monofunctional adduct of **1** or **2** by using Klenow fragments from DNA polymerase I (exonuclease minus, mutated to remove the 3′→5′ proofreading domain; KF$^-$) as a model, which is a well-characterized enzyme frequently used in studies aimed at understanding the processes in which nucleic acid polymerases take part.

We constructed the 8-mer/23-mer primer–template duplexes (Figure 7) unruthenated or containing a single monofunctional adduct of the Ru^{II}–arene complex. The first eight nucleotides on the 3′-terminus of the 23-mer template strand were complementary to the nucleotides of the 8-mer primer so that the 3′ guanine involved in the adduct on the template strand was located at the 14th position from the 3′-terminus (Figure 7A). After annealing the 8-nucleotide primer to the 3′-terminus of the unruthenated or ruthenated template strand (positioning the 3′-end of the primer five bases before the adduct in the template strand), we examined DNA polymerization through the adduct of **1** or **2** by using KF$^-$ in the presence of all four deoxyribonucleoside triphosphates (dNTPs). The reaction was stopped at various time intervals, and the products were analyzed by using a sequencing gel (Figure 7A). Polymerization by KF$^-$ of the 8-mer/23-mer primer templates containing the adduct of **1** or **2** in the presence of all four dNTPs proceeded rapidly up to the nucleotide opposite the ruthenated base, such that the 14-nucleotide intermediate products accumulated to a significant extent (shown in Figure 7A). In particular, there was an extensive accumulation of full-length (23-nucleotide) products from the templates containing the adduct of **2** (Figure 7A, lanes 11–15, and Figure 7B), whereas considerably lower accumulation of full-length products was seen with

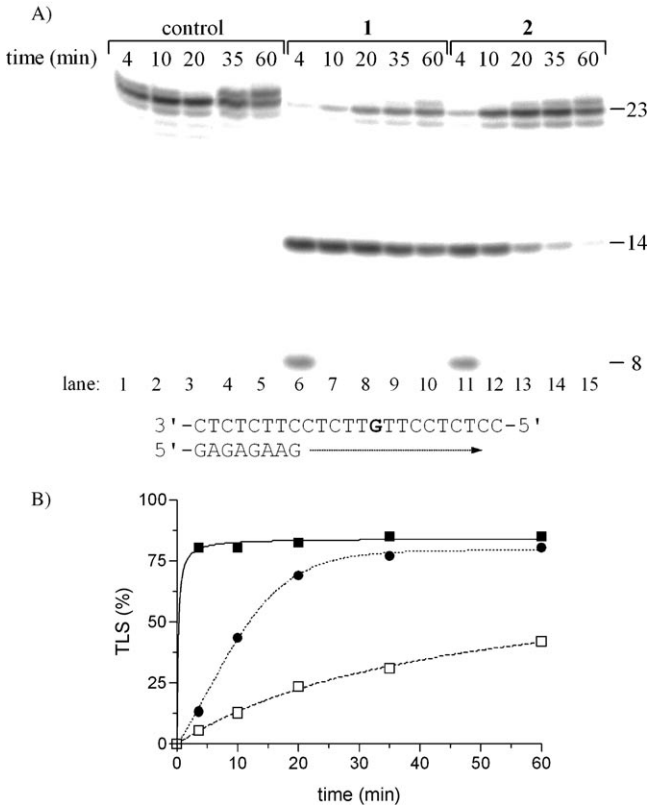

Figure 7. Primer extension activity of KF^-. The experiments were conducted by using the 8-mer/23-mer ("running start" experiment) primer-template duplex for the times indicated. This duplex was unruthenated or contained a single, monofunctional adduct formed by **1** or **2** at the G residue in the TGT sequence. The nucleotide sequences of the templates and the primers are shown below the gels; see the text for details. A) The strong band marked 8 corresponds to the 8-mer primer, the strong pause site opposite the ruthenated guanine is marked 14, and the bands marked 23 correspond to the full-length products. B) The time dependence of the inhibition of DNA synthesis on undamaged (control) template (■), DNA containing the adduct of **1** (□) or **2** (●). Data are means (±SEM) from three different experiments with two independent template preparations.

the template containing the adduct of **1** (Figure 7A, lanes 6–10, and Figure 7B). Only full-length products and no intermediates were seen with the 23-mer unruthenated control template (shown in Figure 7A, lanes 1–5).

Discussion

We have demonstrated in our recent work[13] that the DNA-binding mode of organometallic complex **1**, which is cytotoxic towards tumor cell lines and contains *para*-terphenyl as an arene ligand, involves combined intercalative and monofunctional (coordination) binding, whereas the markedly less cytotoxic complex **2**, which contains a *meta*-terphenyl arene ligand, binds to DNA through mainly a monofunctional coordination to DNA bases. The pharmacological activity of several metallodrugs is modulated by the "downstream" effects of damaged DNA, such as recognition of damaged DNA by specific proteins and/or repair of this damage.[38,39] In addition, distortion of DNA conformation induced by metallodrugs and changes in the thermodynamic stability of DNA induced by the damage represent important factors that affect these "downstream" cellular events.[17,23,40,41] Thus, to assess how these factors might assert themselves in the cellular processing of DNA damage induced by **1** and **2**, we characterized further DNA adducts of these two Ru^{II}–arene complexes by using chemical probes of DNA conformation and ITC. An analysis of conformational distortions induced in DNA by **1** and **2** revealed substantial differences in the character of these distortions. Their analysis by chemical probes of DNA conformation demonstrated (Figure 3) that the distortion induced by the nonintercalating **2** extended over at least 4 bp, whereas the distortion induced by **1** was markedly less extensive and weaker (Figure 3). Thus, these data suggest that the adducts of both **1** and **2** should thermodynamically destabilize DNA and if ruthenium is bound to the central phenyl ring as in **2**, the DNA should be destabilized significantly more than in the case when ruthenium is bound to a terminal phenyl ring as in **1**.

The results of the ITC analysis (Table 1) are consistent with these suggestions. The association constant K for the formation of duplexCAL was reduced markedly less by the adduct of intercalating complex **1** than by the adduct of nonintercalating complex **2** at all temperatures tested. A plausible explanation of this observation is that the intercalators thermodynamically stabilize DNA because they lengthen and unwind DNA, increasing the phosphate spacing along the helix axis.[42,43] Also consistent with the intercalation of **1** and associated smaller thermodynamic destabilization of duplexCAL by the adduct of this complex is the observation that a heat capacity change for formation of the duplexCAL (ΔC_p) that contained an adduct of **1** was markedly more negative than that for formation of the duplexCAL that contained an adduct of **2** ((-632 ± 29) vs. $(-394\pm8)\,J\,K^{-1}\,mol^{-1}$). The analysis in this study cannot address the origins of the observed changes in the ΔC_p values, but the main categories of potential sources can be discussed. One of the major factors responsible for a negative ΔC_p in macromolecular interactions is the burial of nonpolar surfaces upon folding (hydrophobic effect).[44–46] Thus, in the case of formation of an adduct of duplexCAL with **1** or **2**, the burial of hydrophobic base residues and/or aromatic terphenyl ligands might be major forces that determine the extent of the negative heat capacity change for formation of this duplex. Thus, the less-negative value of ΔC_p found for the formation of the adduct of duplexCAL with **2** (compared with that of the adduct with **1**) might be due to the higher accessibility to water of: 1) base residues in the duplexCAL–**2** adduct as revealed by chemical probes of DNA conformation (Figure 3) and consistent with a lower thermodynamic stability of this duplex (Table 1); and/or 2) the nonintercalating aromatic *meta*-terphenyl arene ligand in the adduct with **2**.

Our results demonstrate that there is a distinct difference between the DNA binding modes of **1** and **2**, including the capability of their adducts to affect the conformation and

thermodynamic stability of DNA, and that this difference correlates with the difference in cytotoxicity between the two Ru^{II}–arene complexes.[13] Damage to DNA in cells activates various "downstream" processes that determine biological effects of DNA-damaging agents. Recognition of DNA damage by specific proteins represents the initial step of these processes. The energetics and character of DNA damage can play an important role in defining protein–DNA affinity.[16,47–49] Distortion of DNA has been shown to increase the binding affinity of some proteins,[50,51] presumably by removing the thermodynamic penalty associated with deformation of the DNA double helix. Therefore, we were interested to know whether differences in the properties of DNA modified by **1** and **2** are also reflected by the affinity of DNA adducts of **1** and **2** for two proteins that exhibit distinctly different preferences for high-affinity interactions with damaged double-helical DNA.[52] We examined the affinity of DNA duplexes containing single, site-specific adducts of **1** or **2** for XPA protein and RPA, which have been implicated in the recognition of damaged DNA in mammalian cells.[53]

The results of the present work (Figure 4) demonstrate that the affinity of RPA for a DNA duplex adduct with **1** was markedly lower than for that containing the adduct with **2**. Concomitantly, the adducts of **1** were shown to distort and thermodynamically destabilize DNA much less than the adducts of **2** (Figure 3 and Table 1). Thus, these results are consistent with the known property of RPA, which preferentially binds to heavily distorted DNA, including DNA that contains single-stranded regions, when such a distortion is accompanied by an increased thermodynamic destabilization of DNA, but does not recognize backbone bending.[23,52] On the other hand, XPA protein binds most efficiently to rigidly bent duplexes but not to single-stranded DNA.[52,54] Thus, our observation (Figure 5) that XPA protein does not recognize the DNA adducts of **1** or **2**, but exhibits a high affinity for DNA containing a 1,2-GG intrastrand crosslink of cisplatin (which is known to rigidly bend DNA[55]) apparently has a connection to the inability of monodentate **1** and **2** to rigidly bend DNA.

RPA protein, which discriminates between DNA modified by **1** and **2**, is an indispensable player in almost all DNA metabolic pathways, such as DNA replication, recombination, cell cycle, and DNA repair.[56,57] Moreover, an important feature of the mechanism underlying the antitumor effects of DNA-binding metallodrugs is repair of their DNA adducts.[38,39] A persistence of these DNA adducts might potentiate their antitumor effects in cells that are sensitive to these compounds.[38,39,58,59] DNA repair synthesis was investigated in the present work by using the CFE from human tumor cells and DNA substrates randomly modified by **1** or **2** (Figure 6). Importantly, the adducts of **1** induced a considerably lower level of repair synthesis than the adducts of **2**; this suggests a less efficient removal from DNA and enhanced persistence of the adducts of the more potent and intercalating **1** in comparison with the adducts of less potent and nonintercalating **2**.

Also interestingly, the adducts of **1** inhibit DNA polymerization more efficiently than the adducts of **2** (Figure 7), and they are more difficult for DNA polymerases to bypass. Numerous studies have indicated that the level of DNA adduct tolerance, which has been correlated with the increased ability of DNA polymerases to replicate DNA past metal adducts, inversely correlates with sensitivity to other antitumor metallodrugs, such as platinum drugs.[60,61] In other words, the sensitivity of tumor cells to metallodrugs can be enhanced as a consequence of a lowered adduct tolerance mediated by reduced ability of DNA polymerases to replicate past metal adducts. Herein, we find that DNA adducts of **1** impede elongation of DNA by a model prokaryotic DNA polymerase KF^- to a markedly greater extent than those of **2** (Figure 7). Because there is a high degree of structural and sequence conservation of the domains among DNA polymerases,[62] the results of the studies performed with the KF^- should be also applicable to other (eukaryotic) DNA polymerases.[63–65] Thus, the stronger inhibition of DNA polymerization by the adducts of **1** in comparison with the adduct of **2** might help identify additional factors that explain why the intercalation ability of the arene ligand in monodentate Ru^{II} arene complexes affects processes underlying biological effects of this class of metallodrugs. In addition, the stronger inhibition of DNA polymerization by the adducts of **1** might explain its enhanced cytotoxicity in comparison with **2**.[13] This suggests that chemotherapy based on monodentate Ru^{II} complexes containing arenes that bind to DNA not only through coordination to G N7, but also noncovalently (through hydrophobic interactions between the arene and DNA), might be also less likely (compared with Ru^{II} complexes containing arene ligands incapable of the noncovalent binding) to induce secondary tumors.

Transition-metal-based compounds constitute a discrete class of chemotherapeutics that are widely used in the clinic as antitumor and antiviral agents.[7,66,67] However, drug resistance and side effects have limited their clinical utility. These limitations have prompted a search for more effective and less toxic antitumor metallodrugs. As a part of this search, we and others have been systematically testing a hypothesis that new transition-metal-based drugs that bind to DNA in a fundamentally different manner from that of conventional metallodrugs already used in the clinic might have altered pharmacological properties. This hypothesis was formulated on the basis of the generally accepted fact that DNA is one of the major pharmacological targets of platinum antitumor drugs.[68,69] Some of the efforts motivated by this hypothesis have been also directed toward the design of antitumor ruthenium complexes.[4,70] Although the pharmacological target for antitumor ruthenium compounds has not been unequivocally identified, there is a large body of evidence indicating that the cytotoxicity of several ruthenium complexes in tumor cell lines correlates with the ability of these complexes to bind DNA and affect its properties and cellular processing in a specific way.[5] Results of the present work along with those previously published[8,10–15] further

support the view that monodentate Ru^{II}–arene complexes belong among antitumor ruthenium compounds for which the structure–pharmacological activity relationship may be formulated on the basis of their DNA binding mode. On the other hand, we cannot rule out possibility that the mechanism underlying the cytotoxic activity of monofunctional Ru^{II}–arene complexes involves factors not acting at the DNA level, although experimental data that might support this alternative are as yet lacking.

Experimental Section

Starting materials: Complexes **1** and **2** were prepared by methods described in detail previously.[13] Cisplatin, glycogen, and dimethyl sulfate (DMS) were obtained from Sigma. The stock solutions of ruthenium and platinum complexes in H_2O (5×10^{-4} M) were prepared in the dark at 298 K. Plasmids pUC19 (2686 bp) and pBR322 (4363 bp) were isolated according to standard procedures. The synthetic oligodeoxyribonucleotides were purchased from VBC-Genomics (Vienna, Austria) and were purified as described previously.[71] Restriction endonucleases, T4 polynucleotide kinase, KF^-, and bovine serum albumin were purchased from New England Biolabs GmbH (Frankfurt am Main, Germany). The N-terminal His6-tagged XPA protein was obtained by expressing the plasmid DNA pET15b/XPA template[72] in RTS 500 *E. coli* HY (Roche) and purified on Ni^{2+}–NTA agarose and by hydroxyapatite chromatography.[52] Human recombinant RPA purified from *E. coli*[73] was a kind gift from John J. Turchi. A CFE was prepared from the HeLa S3 cell line as described elsewhere.[74,75] Acrylamide, agarose, bis(acrylamide), ethidium bromide (EtBr), urea, and NaCN were purchased from Merck. Creatine phosphokinase and creatine phosphate were purchased from MP Biomedicals (Irvine, USA). The radioactive products from Amersham were purchased from AP Czech, s.r.o. (Praha, Czech Republic).

Metallation of oligonucleotides: The single-stranded oligonucleotides (the top, pyrimidine-rich strands containing a single central G of the duplexCAL and duplexEMSA, or the template strand used in the studies of DNA polymerization) were reacted in stoichiometric amounts with either **1**, **2**, or cisplatin. The ruthenated or platinated oligonucleotides were purified by using ion-exchange HPLC. We verified that the modified oligonucleotides contained one ruthenium or platinum atom by using ruthenium or platinum flameless atomic absorption spectrophotometry (FAAS) and optical density measurements. We also verified that one molecule of ruthenium or platinum complex was coordinated to the N7 atom of the single G in the pyrimidine-rich strand by using DMS footprinting of ruthenium or platinum on DNA.[76] The strands containing a single, central 1,2-GG intrastrand crosslink of cisplatin were prepared as described elsewhere.[18] The nonmodified, ruthenated, or platinated duplexes used in the studies of recognition by XPA and RPA proteins were purified by electrophoresis on native 15% PAA gels (mono/bis[acrylamide] ratio = 29:1).

Microcalorimetry

Differential scanning calorimetry (DSC): Excess heat capacity (ΔC_p) vs. temperature profiles for the thermally induced transitions of DNA duplexes were measured by using a VP-DSC calorimeter (Microcal, Northampton, MA). In the DSC experiments, the concentrations of the duplexes were 30 μM, the heating rate was 60 K h^{-1}, the maximum temperature was 368 K and the standard buffer for these studies contained NaCl (50 mM) with phosphate buffer (10 mM, Na_2HPO_4/NaH_2PO_4, pH 7.0). After reaching the maximum temperature, the samples were cooled at the same rate to the starting temperature of 288 K.

Isothermal titration calorimetry (ITC): Heat flow during isothermal titration was measured by using a VP-ITC microcalorimeter (MicroCal, Northampton, MA). The standard titration buffer for these studies contained NaCl (50 mM) with phosphate buffer (10 mM, Na_2HPO_4/NaH_2PO_4, pH 7.0). Stock solutions of the strands for ITC studies were prepared in the standard titration buffer and were exhaustively dialyzed against this buffer. For each titration, a solution of the top strand of nonmodified duplexCAL (for the sequence, see Figure 1D) or that containing the single, site-specific monofunctional adduct of **1** or **2** (5×10^{-6} M) in the titration buffer was loaded into the 1.4 mL sample cell and maintained at the selected temperature. A solution of the bottom strand of duplexCAL (5×10^{-5} M) in the titration buffer was loaded into a 300 μL injection syringe. The stirring rate of the injection syringe was 490 rpm and samples were thermally equilibrated until the baseline has leveled off prior to titration. A titration consisted of 50 injections of 5 μL volume and 10 s duration, with 180 s between injections. It was verified that the enthalpies of ITC injections of each individual oligomer into buffer, of buffer into buffer, and of excess oligomer into a solution of duplex were all the same as water into water injections, within the error range. Data from individual titrations were analyzed by using the Origin 5.0 software package (Origin, Northampton, MA) and fitted to a single set of identical sites model to extract the relevant thermodynamic parameters (the enthalpy change (ΔH), entropy change (ΔS), stoichiometry (n), and equilibrium constant (K) for strand association).

Chemical probing of the DNA conformation: The modification of the ruthenated oligonucleotide 15 bp duplexCAL by $KMnO_4$ and DEPC was performed as described previously.[28] The top or bottom strands of the oligonucleotide duplexes were 5′-end labeled with [γ-^{32}P]ATP and T4 polynucleotide kinase. In the case of the ruthenated oligonucleotides, the ruthenium complex was removed after reaction of the duplex with the probe by incubation with NaCN (0.2 M, pH 11) at 318 K for 10 h in the dark.

Reactions with XPA and RPA: ^{32}P-labeled DNA substrates (2.0 nM) and the indicated amounts of XPA or RPA were incubated at 293 K in 15 or 20 μL reactions containing Hepes–KOH (25 mM, pH 8.3), KCl (30 mM), $MgCl_2$ (4 mM), EDTA (1 mM), dithiothreitol (0.9 mM), bovine serum albumin (45 μg mL^{-1}), and glycerol (10%). To assess the binding at equilibrium, reactions were stopped after 30 min by cooling the samples to 273 K. Following addition of gel loading buffer (4 μL) containing Tris–HCl (0.1 M, pH 8.3), glycerol (10%), and orange G (0.05%), the extent of binding was determined on native 6% PAA gels. Electrophoresis was performed for 50 min at 277 K.

DNA repair synthesis by human cell extract: Repair DNA synthesis of CFEs was assayed by using the pUC19 plasmid. Each reaction of 50 μL contained nonmodified pBR322 (600 ng) and nonmodified or ruthenated pUC19 (r_b = 0.03; 600 ng); ATP (2 mM); KCl (30 mM); creatine phosphokinase (rabbit muscle; 0.05 mg mL^{-1}); dGTP, dATP, and TTP (20 mM each); dCTP (8 mM); [α-^{32}P]dCTP (74 kBq) in the buffer composed of HEPES–KOH (40 mM, pH 7.5); $MgCl_2$ (5 mM); dithiothreitol (0.5 mM); creatine phosphate (22 mM); bovine serum albumin (1.4 mg mL^{-1}); and CFE from the HeLa S3 cells (20 mg). Reactions were incubated for 3 h at 303 K and terminated by adding EDTA (to a final concentration of 20 mM), SDS (0.6%), and proteinase K (250 μg mL^{-1}), and then incubating for 20 min. The products were extracted with one volume of 1:1 phenol/chloroform. The DNA was precipitated from the aqueous layer by addition of 3 M NaOAc (0.1 volume) and EtOH (2.5 volumes). After 30 min of incubation at 253 K and centrifugation at 12000 *g* for 30 min at 277 K, the pellet was washed with 80% EtOH (0.2 mL) and dried in a vacuum centrifuge. The DNA was finally linearized prior to electrophoresis on a 1% agarose gel. The resulting gel was stained with EtBr. The experiments were made in quadruplicate.

Inhibition of DNA polymerization: The primer extension assays with all four dNTPs were performed with the 23-mer templates containing a single monofunctional adduct of **1** or **2**. DNA substrates were generated by annealing the 23-mer template containing site-specific adducts of **1** or **2** to the 8-mer 5′-^{32}P-labeled oligomer primer. In the control undamaged DNA substrates, unruthenated 23-mer template was used. The nucleotide sequence of DNA substrate containing 23-mer template oligonucleotides annealed to the primers is shown in Figure 7A. Standard DNA polymerase (KF^-) reactions (50 μL, 298 K) contained Tris–HCl (50 mM, pH 7.4), $MgCl_2$ (10 mM), dithiothreitol (0.1 mM), bovine serum albumin (50 μg mL^{-1}), dNTPs (100 μM), 5′-^{32}P-labeled oligonucleotide primer (40 nM) annealed to an oligonucleotide template, and KF^- (0.5 unit,

6 nM). At various intervals, aliquots (10 μL) were withdrawn, and the reactions in these aliquots were terminated by the addition of loading buffer (5 μL) containing EDTA (20 mM), formamide (80%), bromophenol blue (0.1%), and xylenecyanol blue (0.1%) and by heating at 363 K for 1 min. The reaction products were resolved on 20% PAA gels containing urea (8 M), then visualized and quantified. Other details were published previously.[35,77]

Other physical methods: Absorption spectra were measured by using a Beckman 7400 DU spectrophotometer by using quartz cells with a path length of 1 cm and a thermoelectrically controlled cell holder. The oligonucleotides were purified by HPLC on a Waters HPLC system consisting of a Waters 262 pump, a Waters 2487 UV detector, and a Waters 600S controller with a MonoQ 5/50 GL column. The FAAS measurements were carried out by using a Varian AA240Z Zeeman atomic absorption spectrometer equipped with a GTA 120 graphite tube atomizer. For FAAS analyses, DNA was precipitated with EtOH and dissolved in 0.1 M HCl. The gels were visualized by using a BAS 2500 FUJIFILM bioimaging analyzer and the radioactivity associated with the bands was quantified by using the AIDA image analyzer software (Raytest, Germany).

Acknowledgements

This research was supported by the Ministry of Education of the Czech Republic (MSMT LC06030, 6198959216, ME08017, ME10066, OC08003, and OC09018), the Academy of Sciences of the Czech Republic (grants KAN200200651, M200040901, AV0Z50040507, and AV0Z50040702), the Grant Agency of the Academy of Sciences of the Czech Republic (IAA400040803), and the Grant Agency of the Czech Republic (301/09/H004 and P301/10/0598). J.K. is an international research scholar of the Howard Hughes Medical Institute. The authors also acknowledge that their participation in the EU COST Action D39 has enabled them to regularly exchange their most recent ideas in the field of anticancer metallodrugs with several european colleagues.

[1] R. E. Morris, R. E. Aird, P. D. Murdoch, H. M. Chen, J. Cummings, N. D. Hughes, S. Parsons, A. Parkin, G. Boyd, D. I. Jodrell, P. J. Sadler, *J. Med. Chem.* **2001**, *44*, 3616–3621.
[2] R. Aird, J. Cummings, A. Ritchie, M. Muir, R. Morris, H. Chen, P. Sadler, D. Jodrell, *British J. Cancer* **2002**, *86*, 1652–1657.
[3] Y. K. Yan, M. Melchart, A. Habtemariam, P. J. Sadler, *Chem. Commun.(Cambridge)* **2005**, 4764–4776.
[4] S. J. Dougan, P. J. Sadler, *Chimia* **2007**, *61*, 704–715.
[5] V. Brabec, O. Novakova, *Drug Resist. Updates* **2006**, *9*, 111–122.
[6] M. A. Jakupec, E. Reisner, A. Eichinger, M. Pongratz, V. B. Arion, M. Galanski, C. G. Hartinger, B. K. Keppler, *J. Med. Chem.* **2005**, *48*, 2831–2837.
[7] P. J. Dyson, G. Sava, *Dalton Trans.* **2006**, 1929–1933.
[8] H. Chen, J. A. Parkinson, O. Novakova, J. Bella, F. Wang, A. Dawson, R. Gould, S. Parsons, V. Brabec, P. J. Sadler, *Proc. Natl. Acad. Sci. USA* **2003**, *100*, 14623–14628.
[9] O. Novakova, H. Chen, O. Vrana, A. Rodger, P. J. Sadler, V. Brabec, *Biochemistry* **2003**, *42*, 11544–11554.
[10] O. Novakova, J. Kasparkova, V. Bursova, C. Hofr, M. Vojtiskova, H. Chen, P. J. Sadler, V. Brabec, *Chem. Biol.* **2005**, *12*, 121–129.
[11] M. Melchart, A. Habtemariam, O. Novakova, S. A. Moggach, F. P. A. Fabbiani, S. Parsons, V. Brabec, P. J. Sadler, *Inorg. Chem.* **2007**, *46*, 8950–8962.
[12] S. W. Magennis, A. Habtemariam, O. Novakova, J. B. Henry, S. Meier, S. Parsons, I. D. H. Oswald, V. Brabec, P. J. Sadler, *Inorg. Chem.* **2007**, *46*, 5059–5068.
[13] T. Bugarcic, O. Novakova, A. Halamikova, L. Zerzankova, O. Vrana, J. Kasparkova, A. Habtemariam, S. Parsons, P. J. Sadler, V. Brabec, *J. Med. Chem.* **2008**, *51*, 5310–5319.
[14] T. Bugarcic, A. Habtemariam, J. Stepankova, P. Heringova, J. Kasparkova, R. J. Deeth, R. D. L. Johnstone, A. Prescimone, A. Parkin, S. Parsons, V. Brabec, P. J. Sadler, *Inorg. Chem.* **2008**, *47*, 11470–11486.
[15] O. Nováková, A. A. Nazarov, C. G. Hartinger, B. K. Keppler, V. Brabec, *Biochem. Pharmacol.* **2009**, *77*, 364–374.
[16] N. Poklar, D. S. Pilch, S. J. Lippard, E. A. Redding, S. U. Dunham, K. J. Breslauer, *Proc. Natl. Acad. Sci. USA* **1996**, *93*, 7606–7611.
[17] D. S. Pilch, S. U. Dunham, E. R. Jamieson, S. J. Lippard, K. J. Breslauer, *J. Mol. Biol.* **2000**, *296*, 803–812.
[18] C. Hofr, N. Farrell, V. Brabec, *Nucleic Acids Res.* **2001**, *29*, 2034–2040.
[19] C. Hofr, V. Brabec, *J. Biol. Chem.* **2001**, *276*, 9655–9661.
[20] J. Malina, O. Novakova, B. K. Keppler, E. Alessio, V. Brabec, *J. Biol. Inorg. Chem.* **2001**, *6*, 435–445.
[21] C. Hofr, V. Brabec, *Biopolymers* **2005**, *77*, 222–229.
[22] V. Bursova, J. Kasparkova, C. Hofr, V. Brabec, *Biophys. J.* **2005**, *88*, 1207–1214.
[23] V. Brabec, K. Stehlikova, J. Malina, M. Vojtiskova, J. Kasparkova, *Arch. Biochem. Biophys.* **2006**, *446*, 1–10.
[24] J. Malina, O. Novakova, M. Vojtiskova, G. Natile, V. Brabec, *Biophys. J.* **2007**, *93*, 3950–3962.
[25] O. Nováková, J. Malina, J. Kašpárková, A. Halámiková, V. Bernard, F. Intini, G. Natile, V. Brabec, *Chem. Eur. J.* **2009**, *15*, 6211–6221.
[26] H. K. Liu, S. J. Berners-Price, F. Y. Wang, J. A. Parkinson, J. J. Xu, J. Bella, P. J. Sadler, *Angew. Chem.* **2006**, *118*, 8333–8336; *Angew. Chem. Int. Ed.* **2006**, *45*, 8153–8156.
[27] P. E. Nielsen, *J. Mol. Recognit.* **1990**, *3*, 1–24.
[28] V. Brabec, M. Sip, M. Leng, *Biochemistry* **1993**, *32*, 11676–11681.
[29] H. Kostrhunova, V. Brabec, *Biochemistry* **2000**, *39*, 12639–12649.
[30] S. M. Patrick, J. J. Turchi, *Biochemistry* **1998**, *37*, 8808–8815.
[31] K. M. Comess, J. N. Burstyn, J. M. Essigmann, S. J. Lippard, *Biochemistry* **1992**, *31*, 3975–3990.
[32] Z. Suo, K. Johnson, *J Biol Chem.* **1998**, *273*, 27259–27267.
[33] A. Vaisman, M. W. Warren, S. G. Chaney, *J. Biol. Chem.* **2001**, *276*, 18999–19005.
[34] E. Bassett, A. Vaisman, J. M. Havener, C. Masutani, F. Hanaoka, S. G. Chaney, *Biochemistry* **2003**, *42*, 14197–14206.
[35] J. Kasparkova, O. Novakova, V. Marini, Y. Najajreh, D. Gibson, J.-M. Perez, V. Brabec, *J. Biol. Chem.* **2003**, *278*, 47516–47525.
[36] B. Moriarity, O. Novakova, N. Farrell, V. Brabec, J. Kasparkova, *Arch. Biochem. Biophys.* **2007**, *459*, 264–272.
[37] A. Alt, K. Lammens, C. Chiocchini, A. Lammens, J. C. Pieck, D. Kuch, K. P. Hopfner, T. Carell, *Science* **2007**, *318*, 967–970.
[38] Y. Jung, S. J. Lippard, *Chem. Rev.* **2007**, *107*, 1387–1407.
[39] V. Brabec, J. Kasparkova in *Role of DNA Repair in Antitumor Effects of Platinum Drugs* (Eds.: N. Hadjiliadis, E. Sletten), Wiley, New York, **2009**, pp. 175–208.
[40] G. E. Plum, C. A. Gelfand, K. J. Breslauer in *Physicochemical Approaches to Structural Elucidation: Effects of 3,N4-Ethenodeoxycytidine on Duplex Stability and Energetics* (Eds.: B. Singer, H. Bartsch), International Agency for Research on Cancer, Lyon, **1999**, pp. 169–177.
[41] N. E. Geacintov, S. Broyde, T. Buterin, H. Naegeli, M. Wu, S. X. Yan, D. J. Patel, *Biopolymers* **2002**, *65*, 202–210.
[42] Y. Maeda, K. Nunomura, E. Ohtsubo, *J. Mol. Biol.* **1990**, *215*, 321–329.
[43] M. T. Bjorndal, D. K. Fygenson, *Biopolymers* **2002**, *65*, 40–44.
[44] J. M. Sturtevant, *Proc. Natl. Acad. Sci. USA* **1977**, *74*, 2236–2240.
[45] R. S. Spolar, M. T. Record, Jr., *Science* **1994**, *263*, 777–784.
[46] P. J. Mikulecky, A. L. Feig, *Nucleic Acids Res.* **2004**, *32*, 3967–3976.
[47] W. B. Peters, S. P. Edmondson, J. W. Shriver, *Biochemistry* **2005**, *44*, 4794–4804.
[48] Y. Zhang, Z. Xi, R. S. Hegde, Z. Shakked, D. M. Crothers, *Proc. Natl. Acad. Sci. USA* **2004**, *101*, 8337–8341.
[49] J. Malina, J. Kasparkova, G. Natile, V. Brabec, *Chem. Biol.* **2002**, *9*, 629–638.
[50] R. E. Dickerson, T. K. Chiu, *Biopolymers* **1997**, *44*, 361–403.
[51] S. M. Cohen, E. R. Jamieson, S. J. Lippard, *Biochemistry* **2000**, *39*, 8259–8265.

[52] M. Missura, T. Buterin, R. Hindges, U. Hubscher, J. Kasparkova, V. Brabec, H. Naegeli, *EMBO J.* **2001**, *20*, 3554–3564.
[53] R. Dip, U. Camenisch, H. Naegeli, *DNA Repair* **2004**, *3*, 1409–1423.
[54] Y. Liu, Y. Liu, Z. Yang, C. Utzat, G. Wang, A. K. Basu, Y. Zou, *Biochemistry* **2005**, *44*, 7361–7368.
[55] S. F. Bellon, S. J. Lippard, *Biophys. Chem.* **1990**, *35*, 179–188.
[56] C. Iftode, Y. Daniely, J. A. Borowiec, *Crit. Rev. Biochem. Mol. Biol.* **1999**, *34*, 141–180.
[57] Y. Zou, Y. Liu, X. Wu, S. M. Shell, *J. Cell. Physiol.* **2006**, *208*, 267–273.
[58] J. Kasparkova, J. Zehnulova, N. Farrell, V. Brabec, *J. Biol. Chem.* **2002**, *277*, 48076–48086.
[59] V. Brabec, *Prog. Nucleic Acid Res. Mol. Biol.* **2002**, *71*, 1–68.
[60] E. L. Mamenta, E. E. Poma, W. K. Kaufmann, D. A. Delmastro, H. L. Grady, S. G. Chaney, *Cancer Res.* **1994**, *54*, 3500–3505.
[61] S. W. Johnson, P. B. Laub, J. S. Beesley, R. F. Ozols, T. C. Hamilton, *Cancer Res.* **1997**, *57*, 850–856.
[62] U. Hübscher, H. P. Nasheuer, J. E. Syvaoja, *Trends Biochem. Sci.* **2000**, *25*, 143–147.
[63] W. C. Lam, E. J. C. Van der Schans, L. C. Sowers, D. P. Millar, *Biochemistry* **1999**, *38*, 2661–2668.
[64] T. A. Steitz, *J. Biol. Chem.* **1999**, *274*, 17395–17398.
[65] S. Lone, L. J. Romano, *Biochemistry* **2003**, *42*, 3826–3834.
[66] L. Ronconi, P. J. Sadler, *Coord. Chem. Rev.* **2007**, *251*, 1633–1648.
[67] P. C. Bruijnincx, P. J. Sadler, *Curr. Opin. Chem. Biol.* **2008**, *12*, 197–206.
[68] N. P. Johnson, J.-L. Butour, G. Villani, F. L. Wimmer, M. Defais, V. Pierson, V. Brabec, *Prog. Clin. Biochem. Med.* **1989**, *6*, 1–24.
[69] E. R. Jamieson, S. J. Lippard, *Chem. Rev.* **1999**, *99*, 2467–2498.
[70] E. Alessio, G. Mestroni, A. Bergamo, G. Sava, *Curr. Top. Med. Chem.* **2004**, *4*, 1525–1535.
[71] V. Brabec, J. Reedijk, M. Leng, *Biochemistry* **1992**, *31*, 12397–12402.
[72] C. J. Jones, R. D. Wood, *Biochemistry* **1993**, *32*, 12096–12104.
[73] I. L. Hermanson-Miller, J. J. Turchi, *Biochemistry* **2002**, *41*, 2402–2408.
[74] J. L. Manley, A. Fire, A. Cano, P. A. Sharp, M. L. Gefter, *Proc. Natl. Acad. Sci. USA* **1980**, *77*, 3855–3859.
[75] J. T. Reardon, A. Vaisman, S. G. Chaney, A. Sancar, *Cancer Res.* **1999**, *59*, 3968–3971.
[76] V. Brabec, M. Leng, *Proc. Natl. Acad. Sci. USA* **1993**, *90*, 5345–5349.
[77] O. Novakova, J. Kasparkova, J. Malina, G. Natile, V. Brabec, *Nucleic Acids Res.* **2003**, *31*, 6450–6460.

Received: November 9, 2009
Published online: April 6, 2010

